ELSEVIER

Ceramics International 32 (2006) 647–652

CERAMICS INTERNATIONAL

www.elsevier.com/locate/ceramint

Microwave-assisted synthesis of $PbWO_4$ nano-powders via a citrate complex precursor and its photoluminescence

Jeong Ho Ryu [a,*], Sang-Mo Koo [a], Dong Suk Chang [a], Jong-Won Yoon [a], Chang Sung Lim [b], Kwang Bo Shim [a]

[a] *Department of Ceramic Engineering, Ceramic Processing Research Center (CPRC), Hanyang University, 17 Haengdang-dong, Seongdong-gu, Seoul 133-791, South Korea*

[b] *Department of Advanced Material Science and Engineering, Hanseo University, 360 Daegok-ri, Haemi-myun, Seosan 356-706, South Korea*

Received 22 November 2004; received in revised form 28 March 2005; accepted 24 April 2005
Available online 7 July 2005

Abstract

Nanocrystalline lead tungstate ($PbWO_4$) powders, which have scheelite-type structure, were successfully synthesized at low temperatures using a modified citrate complex method assisted by microwave irradiation. The citrate complex precursors were heat-treated at temperatures from 300 to 600 °C for 3 h. Crystallization of the $PbWO_4$ precursor was detected at 400 °C, and completed at 500 °C. Nanocrystalline $PbWO_4$ powders heat-treated between 400 and 600 °C primarily showed spherical and disperse morphology. The average crystallite sizes of $PbWO_4$ were between 17 and 28 nm at temperatures between 400 and 600 °C, showing a tendency to increase with the temperature. The $PbWO_4$ powders prepared at 600 °C showed the strongest photoluminescent intensity, which was ascribed to the higher crystallinity and homogeneous particle morphology.

Keywords: Microwave-assisted; $PbWO_4$; Nano-powders; Citrate complex precursor; Photoluminescence

1. Introduction

Lead tungstate ($PbWO_4$) has a scheelite-type structure ($I4_1/a$) with a tetragonal unit cell [1]. The structure of Czochralski-grown $PbWO_4$ consists of WO_4 tetrahedra linked to the Pb ions. The first coordination sphere of Pb ions is created by eight oxygen ions in a distorted cube arrangement. The scintillation and luminescence properties of $PbWO_4$ have been intensively studied in the past years [2–6]. At present, there is a strong interest in this material because it satisfies the requirements for modern scintillation detectors in high energy physics [7]. Recently, $PbWO_4$ was selected as a scintillating medium for a new generation crystal calorimeter for the Large Hadron Collider (LHC) project at Conseil Europeen Pour La Recherche Nucleaire (CERN) [8].

Most of the previous approaches for the preparation of $PbWO_4$ required high temperatures and harsh reaction conditions, such as a high temperature solid-state reaction for powders [9] or a hydrothermal method [10]. Lead tungstate thin films have been prepared by reacting various metal oxide thin films with WO_3 vapor [11] and single crystals have been grown from the melt using the methods of Czochralski [12,13] and Bridgman [14]. However, $PbWO_4$ powders prepared by these processes are relatively large with inhomogeneous morphology and composition because WO_3 has a tendency to vaporize at high temperatures [15]. These problems may be solved by applying an advanced wet chemical solution method that employs a citrate complex (modified Pechini method [16]). This method has been used to successfully prepare highly pure powders of various double oxides [17] and various superconductors [18] with multiple cationic compositions.

Microwave irradiation as a heating source has been developed for a number of applications in chemical synthesis

* Corresponding author. Tel.: +82 2 2220 0543; fax: +82 2 2299 2884.
E-mail address: jimihen@ihanyang.ac.kr (J.H. Ryu).

0272-8842/$30.00
doi:10.1016/j.ceramint.2005.04.025

and has also shown how rapid heating rate can be harnessed to produce binary and ternary solid-state compound [19–22]. Compared with the usual methods, microwave-assisted synthesis has the advantages of shortening the reaction time, giving products with small particle size, narrow particle size distribution and high purity. Unfortunately, the exact nature of the interaction of the microwaves with the reactants during the synthesis is somewhat unclear and speculative. However, it is well known that the interaction of dielectric materials, liquids or solids, with microwaves leads to what is generally known as dielectric heating. In liquids, this constant reorientation leads to friction between molecules, which subsequently generate fast homogeneous nucleation and easy dissolution of the gel [19].

Recently, nanometer-sized inorganic materials have attracted much interest from scientists, due to their wide range of optical and electrical properties [23,24]. However, few reports on the synthesis of $PbWO_4$ nanocrystalline powders are found in the literature. In this work, the synthesis of nano-sized $PbWO_4$ powders from citrate complex precursor assisted by microwave irradiation is reported. The precursors and powders were evaluated for the crystallization process, thermal decomposition and particle morphology. Furthermore, photoluminescence of synthesized powders was measured with respect to its effect of the crystallization process and microstructural morphology.

2. Experimental

Lead nitrate ($Pb(NO_3)_2$, Fluka Chemical Co. Ltd., Japan) and ammonium tungstate para pentahydrate ($(NH_4)_{10}W_{12}O_{41}\cdot 5H_2O$, Wako Chemical Co. Ltd., Japan) were used as the metallic cations. De-ionized water (DW) and citric acid ($HOC(CO_2H)(CH_2CO_2H)_2$, CA, Yukiri Pure Chemical Co. Ltd., Japan) were used as the solvent and chelating agent for the process. Fig. 1 shows the flow chart for the synthesis of nano-sized $PbWO_4$ powders using a modified citrate complex method using microwave and conventional heating. The citrate solution was prepared by dissolving appropriate molar ratios of citric acid in de-ionized water (CA:DW molar ratio = 1:4). After complete homogenization of the citrate solution, lead nitrate and ammonium tungstate para pentahydrate were dissolved in the molar ratio of total chelate metal cations (TO) and citric acid (TO:CA molar ratio = 1:5). After heating, the solution is kept at a temperature of 100 °C for 1 h under constant stirring. The solution becomes viscous. A microwave oven with 1200 W (Samsung Electronic Corp., Korea 2.45 GHz) was used to treat the solution. The solution was placed in the microwave oven and the reactions were performed under ambient air for 30 min. The working cycle of the microwave oven was set between 40 s on and 20 s off. The solution became more viscous with time and the color changed to brown. No visible precipitation was observed during the heating process. As this solution condensed, the brown product was converted into powders with a Teflon bar. Thermal analysis was performed on this powder, hereinafter referred to as the 'precursor'. Heat-treatment of the precursor was performed at various temperatures from 300 to 600 °C for 3 h.

The crystallization process of the polymeric precursor was examined by thermogravimetry-differential thermal analysis (TG-DTA, SETRAM, France), using a sample weight of 8 mg and a heating rate of 5 °C/min. The existing phase in the particles after heat-treatment was identified by X-ray diffraction (XRD, Cu Kα, 40 kV, 30 mA, Rigaku,

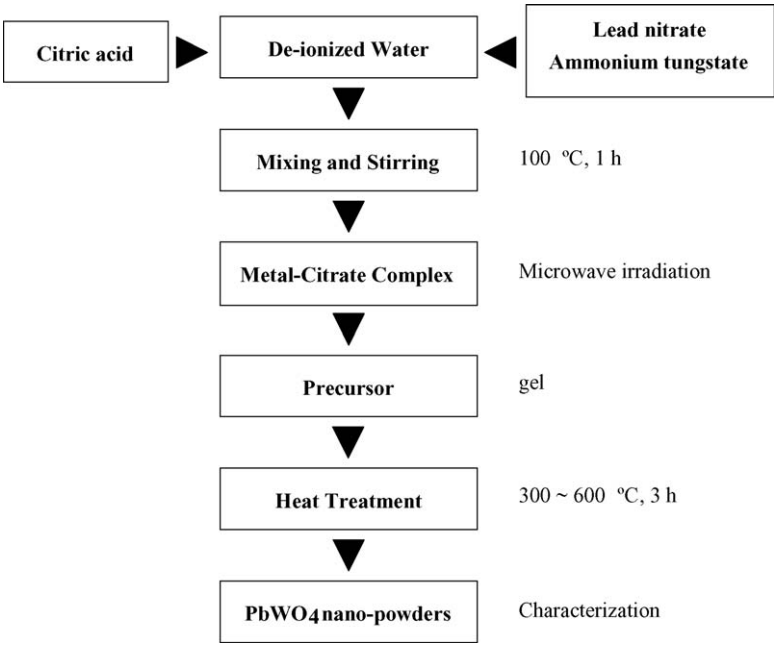

Fig. 1. Flow chart for synthesis of nanocrystalline $PbWO_4$ powders by the modified citrate complex method assisted by microwave irradiation.

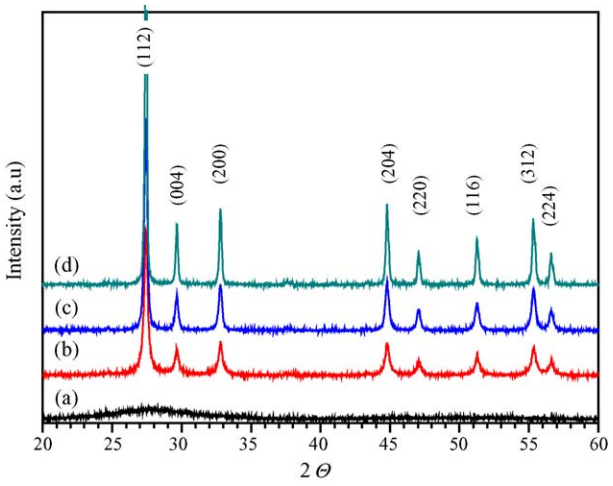

Fig. 2. XRD patterns of the nanocrystalline $PbWO_4$ powders heat-treated at (a) 300, (b) 400, (c) 500 and (d) 600 °C for 3 h.

Japan) with a scan rate of 3°/min. The average crystallite size of the heat-treated powders was calculated by using X-ray diffractometry line broadening method through Scherrer's relationship [25]. The microstructure and surface morphology of the nanocrystalline powders were observed by transmission electron microscopy (TEM, JEM 2010, JEOL). The photoluminescent (PL) spectra were analyzed by a Japan Hitachi 850 Spectrophotometer.

3. Results and discussion

3.1. Synthesis of nanocrystalline $PbWO_4$ powders

The crystallization process of the precursor was evaluated by XRD, TG-DTA and electronic diffraction pattern (EDP). Fig. 2 shows the phase identification of the $PbWO_4$ nanocrystalline powders heat-treated for 3 h as a function of heating temperature in detail using XRD. In Fig. 2(a) the powders of $PbWO_4$ at 300 °C were amorphous with no crystallized phases. Above 400 °C in Fig. 2(b)–(d), the powders were identified as the $PbWO_4$ phase. Unreacted or additional phases were not detected and the crystallinity of the particles increased with heat-treatment temperature. All of the diffraction peaks could be indexed to the tetragonal cell of $PbWO_4$ with lattice constants $a = 5.4521$ Å, $c = 12.0366$ Å, which are consistent with reported values

Table 1
Crystallographic data of $PbWO_4$

	Tetragonal stolzite [26]	Monoclinic respite [1]
Pb-O × N	2.580 × 4, 2.637 × 4	2.65, 2.77, 2.31, 2.68, 2.85, 2.51, 2.47 × 1
Mean Pb–O	2.609 × 8	2.61 × 7
W–O × N	1.795 × 4	2.17, 1.92, 1.97, 2.07, 1.70, 1.83 × 1
Mean W–O	1.795 × 4	1.94 × 6

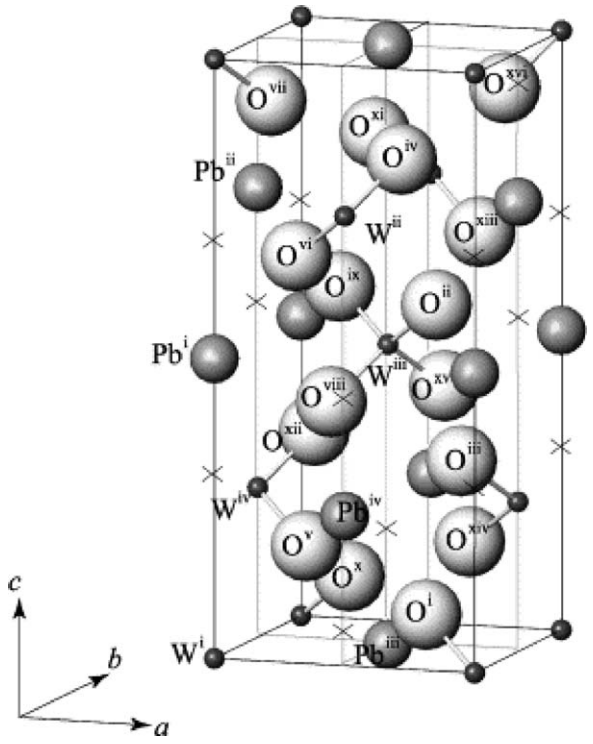

Fig. 3. Schematic view of tetragonal $PbWO_4$. Pb, W and O atoms are represented by middle, small and large spheres, the radii of which are halves of the ionic ones proposed by Shannon for convenience. Symmetry codes for general site are in reference [1]. The 8e site (0 0 z) of $I4_1/a$ symmetry with the equivalent position are depicted by the thin cross marks.

(JCPDS Cards 19-0708). The $PbWO_4$ crystals occur in nature as tetragonal stolzite, scheelite type and monoclinic respite at normal pressure. The crystallographic data for the two types of $PbWO_4$ crystals are shown in Table 1. The XRD results show that the nanocrystalline $PbWO_4$ powders prepared by the citrate complex method have the tetragonal stolzite structure as shown in Fig. 3, where the tungsten atom adopts a tetrahedral coordination.

Fig. 4 shows the TG-DTA curves for the $PbWO_4$ precursor. In Fig. 4, with an increase of temperature, weight loss occurs in the TG curve up to 490 °C. Thereafter the weight remains constant, indicating that the decomposition

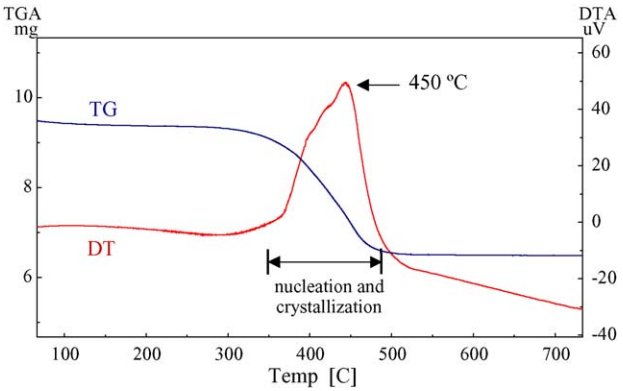

Fig. 4. TG-DTA curves of the $PbWO_4$ precursor in flowing air.

of all organic materials completed in the precursor, their combustion and the crystallization of $PbWO_4$ occurred below 490 °C. No significant plateau corresponding to well-defined intermediate products appeared in the heating process. The DTA curve in Fig. 3 is interpreted as follows: (1) the increase of DTA curve from 350 °C corresponds to the initial decomposition of the precursor and formation of the nuclei of the $PbWO_4$ nanocrystallites; and (2) the exothermic peak at 450 °C corresponds to the crystallization of $PbWO_4$. Below 350 °C, the resultant particles were dark brown and porous in structure. It is attributed to the presence of a lot of carbons and ignitable organics. When the temperature is increased above 350 °C, crystal nuclei begin to form, and consequently the primary crystallization process is completed following the combustion of the residual carbons and ignitable organics.

Fig. 5 shows TEM and electronic diffraction pattern (EDP) of the $PbWO_4$ nanocrystallites prepared from 300 to 600 °C. The EDP of $PbWO_4$ powders heat-treated at 300 °C in Fig. 5(a) shows only diffuse hollow rings, corresponding to an amorphous phase. With the increase in temperature, at 400 °C in Fig. 5(b), dotted rings are observed, signifying the nanocrystalline formation. The TEM morphology in Fig. 5(b)–(d) shows that the sizes of the crystallites gradually increase with the heating temperature. The $PbWO_4$ nanocrystalline powders heat-treated at 400 °C showed primarily co-mixed morphology with spherical and silkworm-like forms. The powders at 500 and 600 °C in Fig. 5 have a relatively spherical and a more homogeneous morphology with a narrow size distribution than those treated at 400 °C.

Table 2
Calculated average crystallite size of $PbWO_4$ powders as a function of heating temperature

Temperature (°C)	Average crystallite size (nm)
400	17
500	23
600	28

The average grain sizes were determined from XRD powder pattern according to the Scherrer's equation [25].

$$D = \frac{k\lambda}{\beta \cos\theta}, \quad (1)$$

where D is the average grain size, k a constant equal to 0.89, λ the wavelength of X-rays equal to 0.1542 nm and β is the corrected half-width that is obtained by using (1 1 1) line of the pure silicon as the standard. Table 2 shows the average crystallite sizes for the heat-treated $PbWO_4$ powders calculated by XRD line broadening method. The calculated

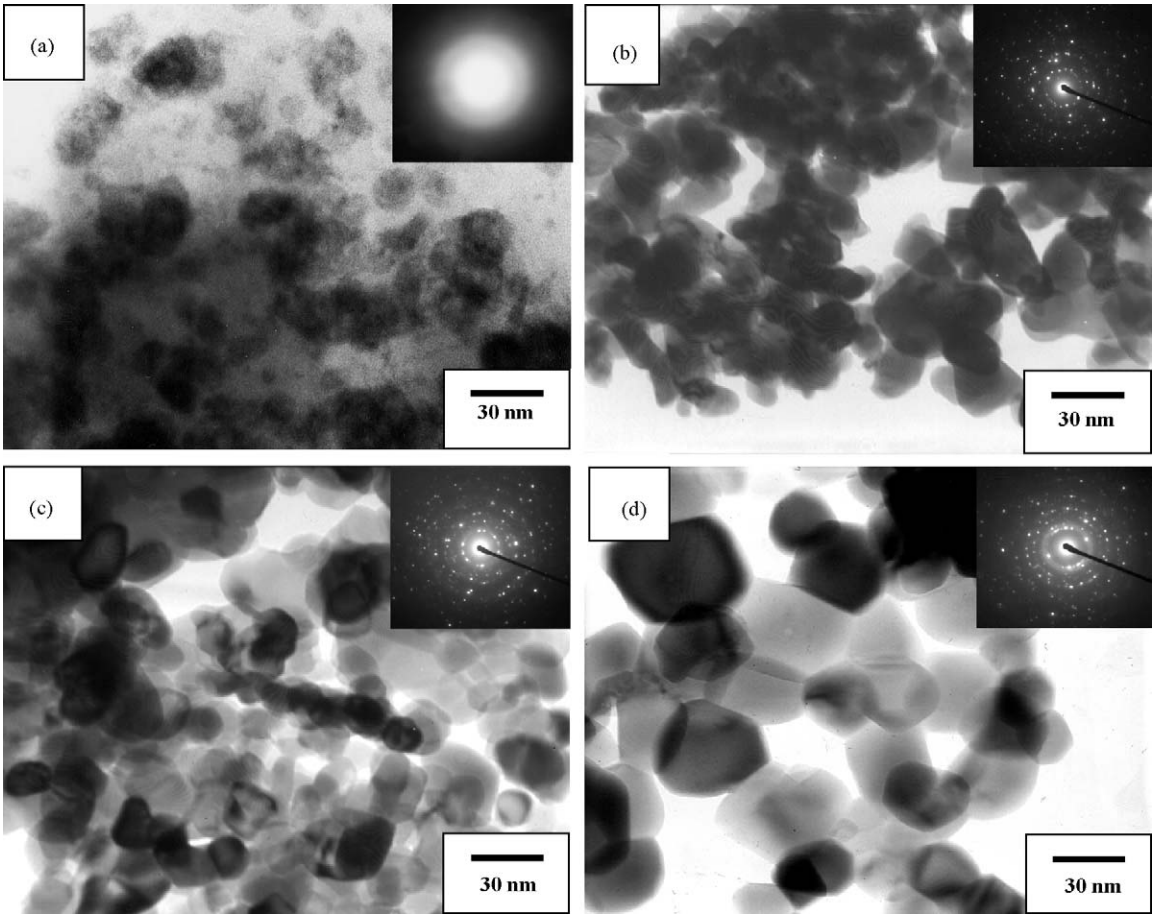

Fig. 5. TEM and EDP of nanocrystalline $PbWO_4$ powders heat-treated at (a) 300, (b) 400, (c) 500 and (d) 600 °C for 3 h.

average crystallite sizes of $PbWO_4$ were between 17 and 28 nm at temperatures range between 400 and 600 °C. These correspond to the TEM observation as shown in Fig. 5 indicating grain growth with increasing temperature.

3.2. Photoluminescence of synthesized nanocrystalline $PbWO_4$ powders

Room-temperature photoluminescent (PL) properties of the prepared nano-sized $PbWO_4$ powders are shown in Fig. 6. The $PbWO_4$ has been identified as intrinsic blue and green luminescence at 400–500 nm with decay time of a few nanoseconds at room temperature, due to the radiative transition of the $[WO_4]^{2-}$ group [27]. It is generally assumed that the measured emission spectrum of $PbWO_4$ is mainly attributed to the charge-transfer transitions within the $[WO_4]^{2-}$ complex [28].

Fig. 6 shows emission spectra of the nanocrystalline $PbWO_4$ powders heat-treated at (a) 400, (b) 500 and (c) 600 °C. With the excited wavelength at 240 nm, the powders exhibited blue emission peaks at 400 nm in Fig. 6(a)–(c), which is a lower wavelength than that of the peaks reported for $PbWO_4$ powders prepared by the hydrothermal method (500 nm [10]) and that of undoped $PbWO_4$ single crystal annealed in air (515 nm [29]). In addition, weak red emission bands near 680 nm were observed. This additional emission band can be ascribed to a defect tungstate tetrahedron [30]. The PL spectrum of samples shown in Fig. 6(a)–(c) have the same maximum peak position. However, the luminescent intensity of sample in Fig. 6(b) and (c) was much stronger than that of sample in Fig. 6(a). The results indicate the dependence of PL properties on the morphology, crystallinity and sizes of the prepared $PbWO_4$ powders. According to literature, the luminescence property of $PbWO_4$ is very sensitive to its structure and strongly relies on structural defects [29]. Generally, it is noted that the synthesizing process for obtaining particles with the shape of a non-agglomerate as well as high crystallinity plays an important role in the improvement of luminescent efficiency [31]. The difference in XRD intensities due to crystallinity of powders causes variations in luminescence efficiency. For similar morphological samples, the homogenized particles must be favorable to luminescent characteristics due to lower contamination or fewer dead layers on the phosphor surface [32,33].

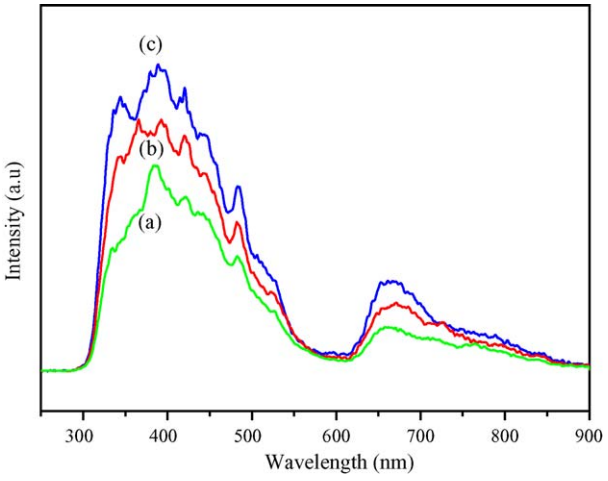

Fig. 6. Emission spectra of the nanocrystalline $PbWO_4$ powders heat-treated at (a) 400, (b) 500 and (c) 600 °C for 3 h.

The enhancement of PL intensity at 500 and 600 °C is ascribed to a higher crystallinity, higher uniformity in particle size distribution, and a more homogeneous particle morphology than of those treated at 400 °C.

4. Summary

The $PbWO_4$ nanocrystalline powders were successfully synthesized using a modified citrate complex method assisted by microwave irradiation. Crystallization of $PbWO_4$ precursor was detected at a low temperature of 400 °C, and completed by 500 °C. The $PbWO_4$ powders heat-treated between 400 and 600 °C showed primarily spherical and homogeneous morphology. The average crystalline sizes of $PbWO_4$ were between 17 and 28 nm at the temperature range between 400 and 600 °C, showing an ordinary tendency to increase with the temperature. The powders prepared at 600 °C showed the strongest photoluminescent intensity, which was attributed to a higher crystallinity, higher uniformity in particle size distribution and more homogeneous particle morphology.

References

[1] S. Takai, S. Touda, K. Oikawa, K. Mori, S. Torii, T. Kamiyama, T. Esaka, Solid State Ionics 148 (2002) 123–133.
[2] J.A. Groenink, G. Blasse, J. Solid State Chem. 32 (1980) 9–20.
[3] W. Van Loo, J. Solid State Chem. 14 (1975) 359–365.
[4] A.A. Annenkov, M.V. Korzhik, P. Lecoq, Nucl. Instrum. Methods Phys. Res. A 490 (2002) 30–50.
[5] Y. Zhang, N.A.W. Holzwarth, R.T. Williams, Phys. Rev. B 57 (1998) 12738–12750.
[6] Y. Chen, C. Shi, G. Hu, J. Appl. Phys. 87 (2000) 1503–1506.
[7] M. Kobayashi, S. Sugimoto, Y. Yoshimura, Y. Usuki, M. Ishii, N. Senguttuvan, K. Tanji, M. Nikl, Nucl. Inst. Meth. A 459 (2001) 482–493.
[8] CMS Technical Proposal CERN/LHCC 94-38, LHCC/P1, 15 December 1994.
[9] G. Blasse, L.H. Brixner, Chem. Phys. Lett. 173 (1990) 409–411.
[10] C. An, K. Tang, G. Shen, C. Wang, Y. Qian, Mater. Lett. 57 (2002) 565–568.
[11] S. Nobuhiro, K. Akihiko, K. Tdayoshi, Bull. Chem. Soc. Jpn. 69 (1996) 1241–1245.
[12] K. Nitsch, M. Nikl, S. Ganschow, P. Reiche, R. Uecker, J. Cryst. Growth 165 (1996) 163–165.
[13] N. Senguttuvan, P. Mohan, S.M. Babu, C. Subramanian, J. Cryst. Growth 183 (1998) 391–397.
[14] K. Tanji, M. Ishii, Y. Usuki, K. Hara, H. Takano, A. Senguttuvan, J. Cryst. Growth 204 (1999) 505–511.
[15] W.S. Cho, M. Yashima, M. Kakihana, A. Kudo, T. Sakata, M. Yoshimura, J. Am. Ceram. Soc. 80 (1997) 765–769.

[16] M.P. Pechini, US Patent No. 3330697, 11 July 1967.
[17] M. Yoshimura, J. Ma, M. Kakihana, J. Am. Ceram. Soc. 81 (1998) 2721–2724.
[18] M. Kakihara, M. Yoshimura, H. Mazaki, H. Yasuoka, L. Borjesson, J. Appl. Phys. 71 (1992) 3904–3910.
[19] C. Jansen, A. Arafat, A.K. Barakat, H. Van Bekkum, in: M.L. Occelli, H. Robson (Eds.), Synthesis of Microporous Materials, vol. 1, Van Nostrand Reinhold, New York, 1992, pp. 507–508.
[20] R. Roy, S. Komarneni, J.L. Yang, J. Am. Ceram. Soc. 68 (1985) 392–395.
[21] I. Teoreanu, E. Andronescu, A. Folea, Ceram. Int. 22 (1996) 305–307.
[22] G.A. Danko, R. Silberglitt, P. Colombo, E. Pippel, J. Woltersdorf, J. Am. Ceram. Soc. 83 (2000) 1617–1625.
[23] G. Schmid, Chem. Rev. 92 (1992) 1709–1727.
[24] A.P. Alivisators, Science 271 (1996) 933–937.
[25] B.D. Cullity, Elements of X-ray Diffraction, second ed., Addison-Wesley Publishing Company, Inc., MA, 1978 , pp. 101–102.
[26] J.M. Moreau, P. Galez, J.P. Peigneux, M.V. Korzhik, J. Alloys Compd. 238 (1996) 46–48.
[27] W. Van Loo, Phys. Stat. Sol. A 28 (1979) 227–235.
[28] V. Pankratov, L. Grigorjeva, D. Millers, S. Chernov, A.S. Voloshinovskii, J. Lumin. 94–95 (2001) 427–432.
[29] C.S. Shi, Y.G. Wei, X.Y. Yang, D.F. Zhou, C.X. Guo, J.Y. Liao, H.G. Tang, Chem. Phys. Lett. 328 (2000) 1–4.
[30] R. Grasser, A. Scharmann, J. Lumin. 12–13 (1976) 473–478.
[31] G.Y. Hong, B.S. Jeon, Y.K. Yoo, J.S. Yoo, J. Electrochem. Soc. 148 (11) (2001) H161–H165.
[32] S.H. Wu, H.C. Cheng, J. Electrochem. Soc. 151 (7) (2004) H159–H163.
[33] Y.C. Kang, H.S. Roh, E.J. Kim, H.D. Park, J. Electrochem. Soc. 150 (4) (2003) H93–H97.